Carbohydrate Polymers 75 (2009) 428–435

Contents lists available at ScienceDirect

Carbohydrate Polymers

journal homepage: www.elsevier.com/locate/carbpol

Characterization and evaluation of hydrophobically modified chitosan scaffolds: Towards design of enzyme immobilized flow-through electrodes

Michael J. Cooney [a,*], Jana Petermann [a], Carolin Lau [a], Shelley D. Minteer [b,*]

[a] Hawaii Natural Energy Institute, University of Hawaii, 1680 East West Road POST 109, Honolulu, HI 96822, USA
[b] Department of Chemistry, Saint Louis University, Saint Louis, MO 63103, USA

ARTICLE INFO

Article history:
Received 15 April 2008
Received in revised form 16 July 2008
Accepted 1 August 2008
Available online 18 August 2008

Keywords:
Chitosan
Scaffolds
Hydrophobic modification
Pore structure
Flow-through electrodes

ABSTRACT

Chitosan scaffolds were fabricated by application of thermally induced phase separation from aqueous solutions of unmodified chitosan and hydrophobically modified chitosan polymer. The final pore structure, in terms of diameter and geometry, were correlated to freezing temperature and freezing time for both the unmodified and hydrophobically modified chitosan polymer. Results showed that the resulting pore structure is strongly dependent upon the freezing temperature and less dependant upon the freezing time. For scaffolds produced from unmodified chitosan, the pore size decreased as expected with decreasing freezing temperature from −5 °C to −10 °C. However, an inconsistency in this trend was observed as the freezing temperature was decreased to −20 °C. Combined analysis of pore size distribution and average pore diameter suggested that the freezing process was mainly mass transfer dominated at −5 °C and −10 °C, but principally heat transfer dominated at −20 °C. In comparison, the scaffolds produced from hydrophobically modified chitosan (butyl-chitosan) followed the expected trend of decreasing mean pore diameter with decreased freezing temperatures throughout the entire temperature range. The scaffolds produced from the unmodified chitosan were more stable and rigid, and possessed average pore diameters that were generally smaller than those fabricated from the hydrophobically modified chitosan. The generally larger pores in the butyl-modified chitosan scaffolds might be explained by increased phase separation rates due to the introduced hydrophobicity of the chitosan polymer. Among the scaffolds fabricated from the butyl-modified chitosan, those produced at −20 °C yielded the most uniform pore structure, the smallest average pore diameters, and the least temporal broadening of pore size distribution.

1. Introduction

Chitosan [Poly-(1→4)-β-D-glucosamine CS] is a derivative of chitin (Gu, Xue, & Li, 2001), a widely available and abundant polysaccharide that occurs naturally in arthropod exoskeletons (Madihally & Matthew, 1999) and insects (Klotzbach, Watt, Ansari, & Minteer, 2008). Chitin, a linear, crystalline, basic and hydrophobic polysaccharide, is formed into chitosan through its partial N-deacetylation (Klotzbach et al., 2008; Dutta, Ravikumar, & Dutta, 2002). When placed in dilute acids at pH below its pKa (6.3), the free amino groups become protonated and a high charge density, which allows the polymer to form ionic complexes with a wide variety of water soluble polyanionic species, forms and the polymer becomes soluble (Madihally & Matthew, 1999). The protonated amino groups along the polymeric backbone give chitosan its polyelectrolyte behavior (Klotzbach, Watt, Ansari, & Minteer, 2006). In basic aqueous solution (pH > 7), however, the free amino groups are no longer protonated and the polymer becomes insoluble.

Chitosan is a biodegradable, nontoxic and biocompatible material that can be fabricated into macroporous and highly interconnected pore structures for use in tissue engineering and slow release drug delivery systems (Leffler & Muller, 2000). Chitosan doped with multi-walled carbon nanotubes has also been used to create highly porous conductive scaffolds (Lau, Cooney, & Atanassov, 2008). It can also be modified by the addition of hydrophobic alkyl chains along the hydrophilic backbone of the chitosan polymer. The combination of hydrophobic groups juxtaposed along an otherwise hydrophilic backbone creates internal forces that tend to fold or buckle the polymer chain, creating mesopores or "regions" that exhibit micellar behavior (Esquenet, Terech, Boue, & Buhler, 2004; Jiang, Quan, Liao, & Wang, 2006). These regions have been shown to provide good enzyme retention and lifetime without loss of activity. Although chitosan modified with small alkyl chains (i.e., <4 carbon chain length) is soluble in dilute aqueous acetic acid although the introduction of longer chain side groups

* Corresponding authors. Tel.: +1 808 956 7337; fax: +1 808 956 2336.
E-mail addresses: mcooney@hawaii.edu (M.J. Cooney), minteers@slu.edu (S.D. Minteer).

0144-8617/$ - see front matter © 2008 Elsevier Ltd. All rights reserved.
doi:10.1016/j.carbpol.2008.08.008

renders the modified polymer relatively increasingly less soluble in dilute acidic aqueous solution (Klotzbach et al., 2006).

A number of other techniques (including freeze-gelation and cross-linking) have been proposed and the effects of process parameters on pore diameter characterized, (Hsieh et al., 2007), in this work we have applied the technique of thermally induced phase separation (Cooney et al., 2007). When a chitosan solution is exposed to subfreezing temperatures, the process of thermally induced phase separation occurs (TIPS). In general, ice crystals nucleate and grow in layers, dehydrating the aqueous chitosan phase until a dense precipitate is formed around the solid ice crystals. The final scaffold structure is achieved after the water is sublimed away, with the actual shape of the now evaporated ice crystals determining the final scaffold pore structure. With respect to freezing time, it has been reported that under mass transfer dominated regime, the final ice crystal size, in terms of its mean radius, will increase with increased freezing time (Cooney et al., 2007) and (Khvorostyanov & Curry, 2004). This experimental observation is suggested to result from the fact that at the higher freezing temperatures (e.g. lower ΔT gradient) the rate of nucleation and subsequent survival of ice crystal embryos is lower. Since the amount of available water that will ultimately diffuse out of the chitosan phase to feed the crystal growth remains constant, a fewer number of larger ice crystals is achieved.

Currently there is no literature describing the pore structure of scaffolds that would be produced from hydrophobically modified chitosan, although there are recent interesting contributions to the preparation, characterization, and aggregation behavior of amphiphilic chitosan derivatives having poly(L-lactic acid) side chains (Li, Zhuang, Mu, Wang, & Fang, 2008). In theory, they are expected to possess a slightly different macropore structure, partially, because the introduction of the hydrophobic alkyl side chains is expected to alter the polymers solubility and viscosity within aqueous solution. Since the phase separation process is affected by the viscosity of the solution (Roh & Kwon, 2002), the crystal structure, dimension and orientation is therefore expected to be influenced by the introduction of increased hydrophobicity and viscosity of the chitosan polymer. For example, the averaged mean diameter of the macrospores might be smaller for scaffolds fabricated from hydrophobically modified chitosan (as opposed to those fabricated from non-modified chitosan) material due to reduced mass transfer rate of the liquid phase out of the polymer caused by a higher viscosity that retards phase separation rates.

The authors have previously shown that enzyme catalyzed electrodes fabricated from butyraldehyde modified chitosan demonstrated greater power density when made in the scaffold structure as opposed to thin films (Cooney et al., 2007). In order to evaluate the capacity of this proof of principle finding to be scaled up into 3D "flow-through" electrodes, this study characterizes the pore structure of hydrophobically modified chitosan and compares them against those made from unmodified chitosan.

2. Experimental

2.1. Chemicals

Butyraldehyde (Fluka 4500266), low molecular weight chitosan (Aldrich, Cat No. 44, 886-9; 75–85% deacetylation), concentrated acetic acid (Fisher Scientific, Lot No.041806), methanol (Fisher A412-4), NaH_2PO_4 (Fisher S381-500), Na_2HPO_4, (Fisher S373-500), sodium cyanoborohydride (Fluka 2589-60-7), and *t*-amyl alcohol (SIGMA 152463) were purchased and used as delivered. Phosphate buffer solution was made by preparing 0.1 M stock solutions of NaH_2PO_4 and Na_2HPO_4 and mixing each as appropriate to achive a pH of 7.15 and by adding water to achieve a final concentraiton of 0.05 M.

2.2. Hydrophobic modification of chitosan

Chitosan was hydrophobically modified by a reductive amination reaction in which the carbonyl group of an aldehyde is reacted with the amine group of the chitosan, forming an intermediate imine, which was subsequently reduced to an amine by cyanoborohydride. Specifically, 0.5 g of chitosan was dissolved in 15 mL of 0.17 M HOAc under rapid stirring. 15 mL methanol was then added to the viscous gel-like solution. The gel was the stirred for 15 min before 20 mL butyraldehyde was added. The mixture was allowed to stir for 5 min before 1.25 g of sodium cyanoborohydride was added to catalyze the reduction of the imine. The gel was then continuously stirred until the suspension returned to room temperature. The resulting product was separated by vacuum filtration and washed with 150 mL increments of methanol. The modified chitosan was then dried in a vacuum oven at 40 °C for 2 h, leaving a flakey white solid. To prepare 1 wt.% solutions of dissolved chitosan for scaffold formation, 0.02 g of the modified polymer was then suspended in 2 mL of 0.2 M acetic acid. We did not resuspend the modified chitosan in *t*-amyl alcohol as per (Klotzbach et al., 2006) as were unable to obtain scaffolds with such solutions after the freezing and freeze drying process.

2.3. Scaffold fabrication

400 μL of polymer solution (1 wt.% chitosan or 1 wt.% butyl-modified chitosan, respectively, in 0.2 M HOAc, pH 2–3) were mixed with 200 μL phosphate buffer (PB) (0.05 M, pH 7.15) to a final ratio of 2:1 (final weight percent of 0.6 wt.% polymer) in order to mimic the addition of enzyme solution (PB) to the polymer. The solution was vortexed for 30 s and then placed into a precooled aluminum mold (4 °C) with four 100 μL pockets. The mold was then placed onto a thermoelectric cooling plate and the setpoint set to −20 °C for 10 min, 30 min, 1 h, 3 h, and 5 h. In general it took 2 min for the solution to reach −20 °C (data not shown). The frozen gel was then freeze dried for at least 2 h until a fully dehydrated scaffold was achieved. The experiment was repeated for freezing temperatures of −20, −10 and −5 °C.

2.4. Scanning electron microscopy

Freeze dried scaffolds were carefully cut into halves using razor blades and the cross sections were then attached onto SEM studs using conductive tape. The samples were then sputter-coated with gold-palladium for 50 s (Hummer 6.2) prior to placement into the SEM chamber (Hitachi S-800) where an accelerating voltage of 10 kV was used to take images at various levels of magnification.

2.5. NMR

Chitosan samples (typically between 30 and 40 mg dry weight) were dried over night under vacuum and the ^{13}C spectrum was determined in the solid state using a Varian Inova 400 WB operated at a H-1 frequency of 399.992 mHz. Samples were spun at a rotation speed of 8 kHz and at 54.7° (the magic angle). Spectra were recorded using cross polarization (CP) at a γ^*B1 field of 50 kHZ for the polarization transfer and high power ^1H decoupling was applied during data acquisition using a γ^*B1 field of 75 kHz.

2.6. Data analysis

Pore size diameter was characterized through software assisted examination of SEM images (Image J, NIH, USA). The pore diameter was estimated with respect to both the vertical and parallel axes by averaging the pore diameter $\bar{d}$ over both the pore length L and width W as described in Eq. (1):

$$\bar{d} = \frac{\sum_{i=1}^{n} d_i^L + d_i^W}{n} \quad (1)$$

where n is summed over all diameters (L and W). The associated standard deviation σ was calculated where the value of n was at least 100 points. The individual pore diameters (as calculated by summing its length L and width W) were also plotted in histograms (Fig. 2) where the histogram peak depicts the averaged pore diameter $\bar{d}$ and the peak broadening taken to represent the standard deviation σ of the average (Fig. 2).

3. Results and discussion

3.1. Verification of hydrophobic modification

NMR measurements (Fig. 3) were executed on modified chitosan samples to verify the successful binding of the hydrophobic alkyl groups (butyraldehyde) to the amine during the reaction. Specifically, 75% deacetylated chitosan was modified and the resulting structure examined with NMR. The NMR spectra for chitosan modified with butyraldehyde are presented in Fig. 3. In all spectra the chemical shifts at 174 ppm and 23 ppm belong to the carbonyl carbon and the methyl group of the acetamine group, which signal heights depend on the degree of deacetylation of the original product chitin. The ratio of ^{13}C signal fits to the theoretical degree of deacetylation as addressed by others in the literature (Heux, Brugnerotto, Desbrieres, Versali, & Rinaudo, 2000; Methacanon, Prasitsilp, Pothsree, & Pattaraarchachai, 2003). The chemical shifts at 105, 84, 76, 60 and 56 ppm were assigned to the ring carbons, C-1, C-4, C-3 and C-5, C-6 and C-2. The modification of the amine group by attaching a butyl group (see Fig. 1) should not have a huge influence on these chemical shifts. In fact only the C-2, as next attached carbon is shifted a bit downfield. The chemical shift at 50 ppm can be defined as the first alkyl carbon, followed by the remaining four alkyl carbon atoms at lower ppm, respectively. This NMR data confirms the reductive amination reaction was successful at hydrophobically modifying the chitosan.

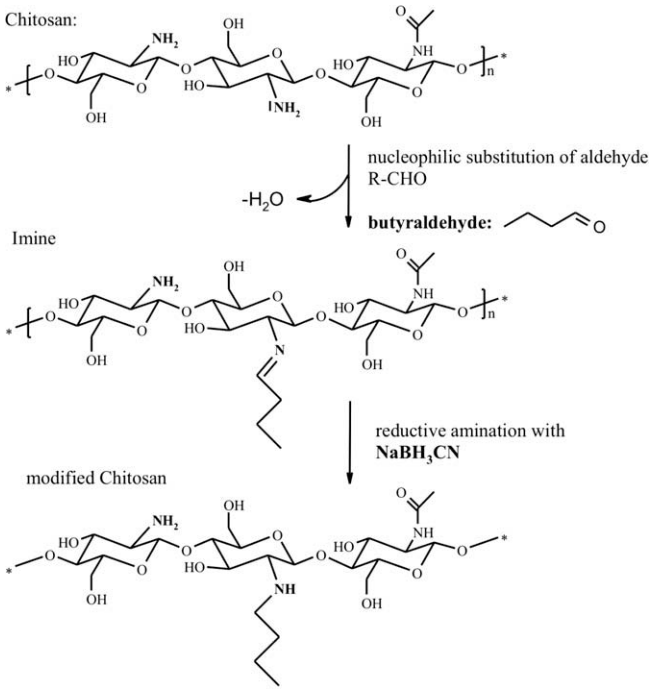

Fig. 1. Reaction mechanism for the reductive amination of chitosan.

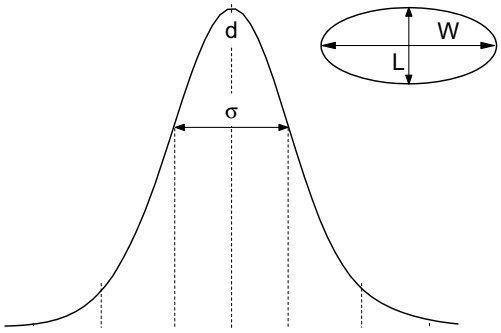

Fig. 2. Terms for statistical analysis of pores.

3.2. General description of ice crystal growth and its relation to scaffold pore structure

Ice crystal growth is largely a three stage process. In the first stage, termed nucleation, an ice crystal nucleus is formed after a specific mass of super-cooled water crystallizes. In the second stage, termed growth, liquid phase water molecules diffuse to the outer surface of the ice nucleus where they freeze, permitting the ice crystal to grow in layers and in relative isolation of other ice crystals. In the third and final stage, termed ripening, ice crystal growth can either occur through the process of Ostwald's ripening, in which one ice crystal grows at the expense of a second, whose outer layer melts and thereby frees up liquid phase water molecules that can migrate via molecular diffusion, or by the process of abutment, whereby by two ice crystals grow into one another, thus forming a single larger ice crystal.

After nucleation, only those ice nuclei that are kinetically favored will survive and grow (the remainder, too small to surpass a critical surface to volume ratio, will dissolve and return to the liquid phase). The nucleation event can be either instantaneous or progressive with the difference impacting the final pore structure. With instantaneous nucleation, the majority of the ice crystal nuclei are formed over a period of time that is *short* relative to the total time period of ice crystal growth (Penner, 2001). Thus, those nuclei that survive will grow for roughly the same amount of time, under the same conditions, and will therefore achieve roughly the same final shape. Consequently, the distribution of ice crystal size (i.e. as measured by their diameter) will not vary significantly during the growth phase regardless of whether this occurs under mass or heat transfer dominated regime – so long as that single regime remains dominate throughout the growth process.

With progressive nucleation, by contrast, the nucleation of ice crystals continues for a given length of time that is *significant* relative to the total time period of ice crystal growth (Penner, 2001). Depending upon whether the phase separation process is mass or heat transfer dominated, the final distribution of ice crystal size can vary significantly during the growth phase. When mass transfer dominated, ice crystal growth is kinetically controlled and the growth rate is constant with time, and the ice crystal size distribution at the end of growth will mirror the size distribution that existed at the end of the progressive nucleation stage – assuming it ended before growth ended. In general this means that the ice crystal size distribution will widen during growth until the end of the progressive nucleation stage, at which point the distribution will remain constant until ice crystal growth terminates. When the phase separation process is heat transfer dominated, ice crystal growth process is diffusion controlled and the ice crystal growth rate will be proportional to the negative square root of time ($t^{-1/2}$). Under these conditions the growth rate of any given ice crystal will be its most rapid immediately after nucleation and thereafter decrease exponentially with time. In general this means

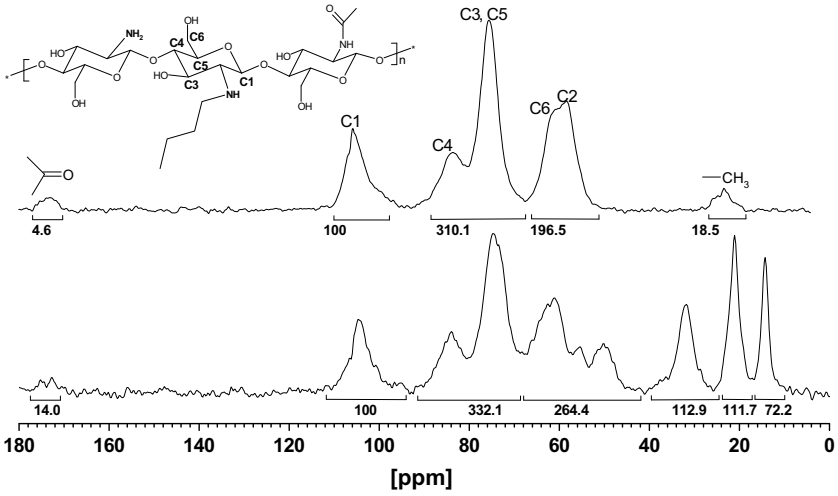

Fig. 3. ^{13}C NMR spectra of non-modified chitosan and butyl-chitosan.

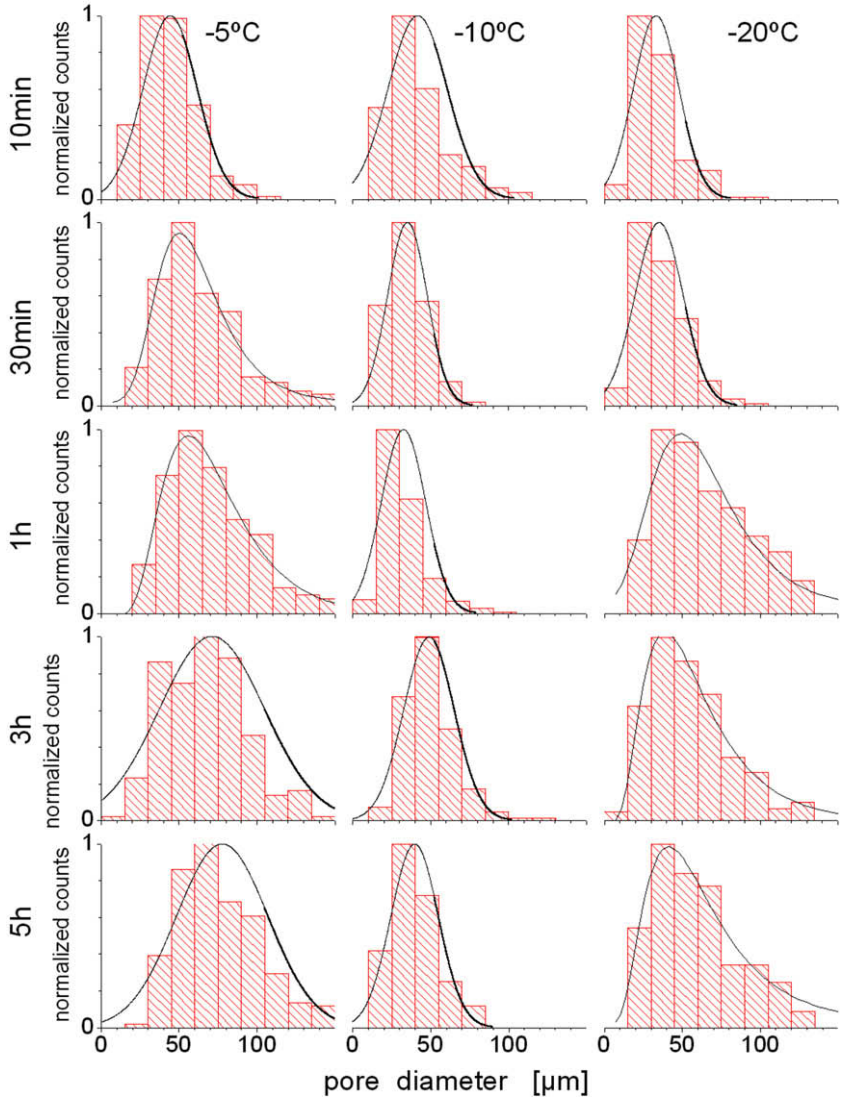

Fig. 4. Histograms of the pore diameter distribution for the scaffolds produced from non-modified chitosan at different temperatures ($T = -5, -10, -20$ °C) and at different freezing times.

that the younger and smaller ice crystals, which grow faster, will tend to catch up in size with the larger ice crystals, which grow slower, and the ice crystal size distribution will narrow until the growth phase has terminated.

The last stage after growth is the ripening stage during which the ice crystal size and distribution can be altered by one of two processes. In the first, known as Ostwald ripening, larger ice crystals grow at the expense of smaller neighboring ice crystals that shrink, through the molecular transfer of water molecules from the shrinking to the growing ice crystals. In general, this broadens the size distribution, almost towards a somewhat equal bimodal distribution, in which one distribution spreads around a population of shrinking ice crystals while the other spreads around a population of growing crystals. In the second, known as coalescence, the ice crystals actually grow into each other until they abut and coalesce, thereby creating one larger ice crystal out of two smaller ones. This can also broaden the size distribution, but in a manner whereby the broadening largely occurs towards the presence of larger ice crystals and with a disappearance of smaller ice crystals.

3.3. Effect of freezing time and temperature on pore structure in scaffolds fabricated from unmodified chitosan

To evaluate the effect of freezing time and temperature on chitosan pore structure, chitosan was dissolved in 0.2 M acetic acid 1 wt.% and this solution mixed with 0.05 M pH 7.15 phosphate buffer in a 2:1 ratio and the mixture frozen for various lengths of time at various temperatures. The pore diameter distribution, measured over at least 100 pores, is presented in Fig. 4 as a function of freezing time for freezing temperatures of −5, −10, and −20 °C. From these histograms, the averaged pore diameter, $\bar{d}$, is extracted and reported in Fig. 5a. The results showed the expected trend of decreased average pore diameter as the freezing temperature decreased from −5 to −10 °C. The expectation comes from the observation that at lower freezing temperatures (e.g., −10 versus −5 °C) more of the newly formed ice crystal nucleates will survive, leading to a greater number of smaller ice crystals (assuming the total amount of water available is fixed). In other words one can expect a trend of decreasing average pore diameter with decreasing freezing temperature, assuming ice crystal growth occurs under mass transfer dominated regime (i.e., the ice crystal growth is kinetic controlled) – which is generally predicted to occur at the higher freezing temperatures (i.e. −5 °C as opposed to −80 °C). In our work, this trend continued as the freezing temperature was dropped to −20 °C, but only for a freezing time of 30 min. For freezing times beyond 30 min, a sudden "step" increase in the average pore diameter was observed. This data reflects a "step" change in the pore size distribution that reflects a shift in the phase separation process from mass to heat transfer dominated. This suggests that for our system the transition occurred at around −20 °C, which is in contrast to the predicted transition temperature of −50 °C suggested by (Roh & Kwon, 2002). Bear in mind, though, that the work of Roh and Kwon studied the freezing of chitosan scaffolds in much larger molds and reduced heat transfer, a factor that likely explains the discrepancy.

Further insight into the ice crystal growth can be considered by plotting the pore size distribution (as represented by the standard deviation of each histogram) as a function of freezing time for each freezing temperature (Fig. 5b). Across all freezing temperatures there is little time dependent variation in the distribution of measured pore diameters except for the previously observed single "step" transition that occurred at 30 min for the scaffolds frozen at −20 °C. Such lack of variation in pore size distribution (excluding the single "step increase) suggests that instantaneous nucleation of ice crystals occurred across all conditions, but that the "step" change that occurred at 30 min was solely a result of the phase separation process changing from mass to heat transfer dominated. The result of instantaneous nucleation is assumed reasonable because the volume of solution being frozen in all cases was only 100 μl and because the solution was contacted on five sides by a relatively good conductor of heat (i.e., alumina).

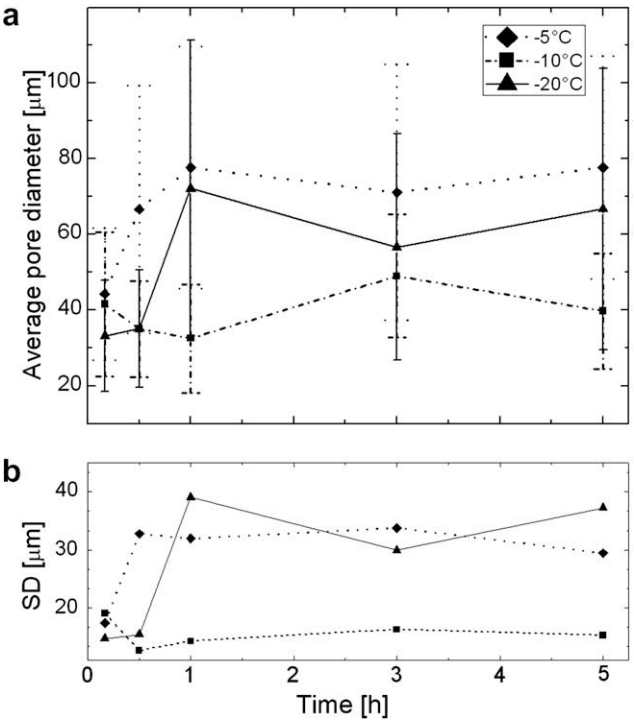

Fig. 5. (a) Averaged mean pore diameter for scaffolds produced from unmodified chitosan in 0.2 M HOAc and 0.6 wt.% chitosan. Legends: diamonds −5 °C; squares −10 °C; triangles −20 °C after the repetition of the sample −20 °C 1 h, −20 °C 3 h and −5 °C 30 min. The averaged pore diameter $\bar{d}$ was taken as the sum of all measured diameters divided by the total number of pore measured. (b) Pore size distribution as a function of freezing temperature and time for scaffolds fabricated from unmodified chitosan.

The observed transition from mass to heat transfer dominated regime can also be characterized by a "step" shift in the pore geometry – assuming thermal gradients exist. As our molds contact the solution on five sides, but leave an insulating air-inter-

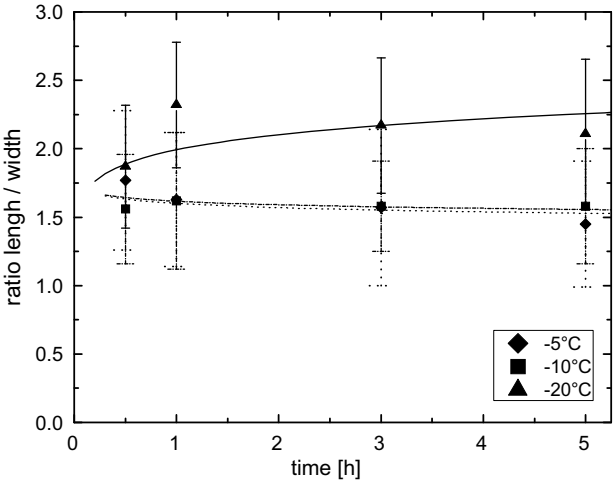

Fig. 6. Ratio of pore length to width for unmodified chitosan as a function of freezing time and temperature. Symbols: diamonds −5 °C, squares −10 °C, triangles −20 °C.

face along the surface, the development of lateral thermal gradients is expected. Consequently, under heat transfer dominated regime one would expect a shift in pore geometry from one that is spherical to one is that longitudinal, as has been observed in similar chitosan systems where uni-directional temperature gradients were imposed (Roh & Kwon, 2002). These kinds of shifts can be observed by plotting the length to diameter ratio (L/W, see Fig. 2) as a function of freezing time and temperature. As can be seen in Fig. 6, which presents this transition for those scaffolds frozen at −20 °C, such a transition occurred at a freezing time of 30 min.

3.4. Effect of freezing time and temperature on pore structure in scaffolds fabricated from hydrophobically modified chitosan

To investigate the effect of introducing hydrophobic side chains along the backbone of hydrophilic chitosan polymer, scaffolds were fabricated from hydrophobically modified chitosan and their final macropore structure characterized in terms of averaged pore diameter. As with the unmodified scaffolds, the raw data is presented as histograms (Fig. 7) and the average pore diameter was plotted over time (Fig. 8a).

The scaffolds produced from the hydrophobically modified chitosan possessed, for a given freezing time, smaller average pore diameter when frozen at a lower freezing temperatures (i.e. −20 versus −5 °C). This suggests that ice crystal growth occurred under mass transfer dominated regime across all freezing temperatures and time, and was absent the "step" transition from mass to heat transfer domination at −20 °C as found for the non-modified chitosan. This is likely due to the fact that the hydrophobically modified chitosan has more mass (i.e. the additional alkane side chains) that are not thermally conductive. In this scenario, the heat transfer conductivity (the rate at which the solution freezes) will be reduced, suggesting that one effect of the hydrophobic transition is to seemingly lower the freezing temperature at which a transition from mass transfer to heat transfer dominated regime occurred.

As with the non-modified scaffolds, the distribution of the pore diameter as function of time for three different freezing temperature is plotted in Fig. 8b. For scaffolds fabricated at freezing times of −5 and −10 °C the distribution of macropore diameters is non-linear with respect to freezing time. At −5 °C the distribution initially narrows until re-widening at the longest freezing time (5 h), while at −10 °C, the non-linearity (although less distinct) begins to widen at later freezing times (3 and 5 h). At −20 °C the non-

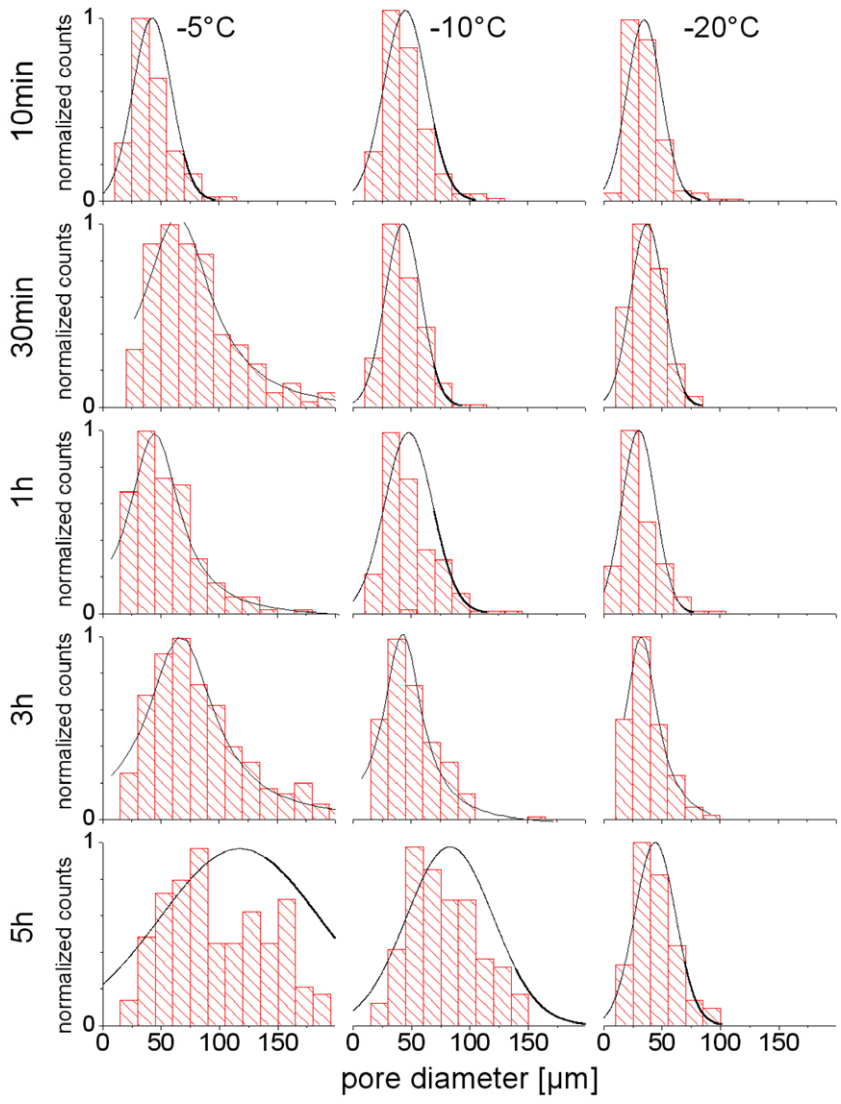

Fig. 7. Histograms of the pore diameter distribution for the scaffolds produced from butyraldehyde modified chitosan (butyl-chitosan) at different temperatures (T = −5, −10, −20 °C) and at different freezing times.

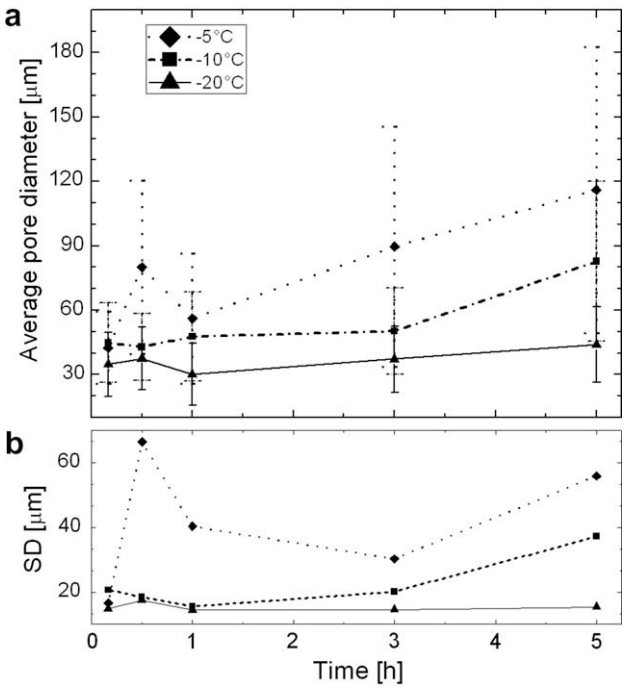

Fig. 8. (a) Average pore diameter of resulting scaffolds from butyl-chitosan in dependence of different freezing times and temperatures. Symbols: diamonds −5 °C, squares −10 °C, triangles −20 °C. (b) Average pore diameter distribution over time for scaffolds produced from butyl-chitosan with linear trend line.

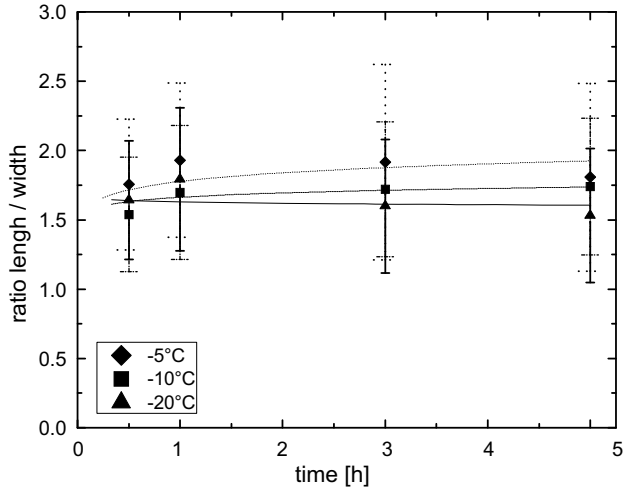

Fig. 9. Ratio of mean pore length to width of scaffolds from butyl-chitosan in dependence of freezing time and temperature. Symbols: diamonds −5 °C, squares −10 °C, triangles −20 °C.

linearity is nonexistent across all freezing temperatures and time disappears, as was found for the unmodified scaffolds. The presence of non-linearity in the macropore diameter distribution generally suggests progressive, as opposed to instantaneous, nucleation. From our results, progressive nucleation is more pronounced at higher freezing temperatures, where the ΔT gradient driving the freezing process is the lowest, but absent at the lowest freezing temperature (−20 °C) where the ΔT gradient is the highest. This makes sense for a system where the heat transfer rate through the system has been retarded by modifications to the soluble polymer.

The macropore length-to-height ratio is plotted in Fig. 9. In general the ratios fall within the values calculated for the unmodified scaffolds except that a sharp transition at −20 °C is not observed, further supporting the assumption that the shift from mass to heat transfer dominated regime did not occur for the modified chitosan at any freezing temperature. More, the lack of any significant variation in the ratio suggests that pore elongation was not significant.

The average pore diameters for scaffolds produced at −5 °C were generally larger for the hydrophobically modified chitosan scaffolds, a trend that was particularly accentuated at the longest freezing time, 5 h. For the freezing temperature of −20 °C, the results were similar only at the shortest freezing time (30 min), after which the trend was dramatically different: the macropore diameters of the unmodified scaffolds were much larger at higher freezing times, and this change correlated to the transition from mass transfer to heat transfer dominated regime. In summary, under mass transfer dominated regime, the effect of hydrophobically modifying the chitosan was to seemingly extend the conditions of mass transfer dominated growth by raising the freezing temperature (i.e. and lowering ΔT) and therefore mimicking the situation (assuming a fixed amount of total water in the systems) where fewer ice nucleates survive but each ultimately grow larger.

3.5. Physical observations and anecdotal comments

Scaffolds fabricated from solutions of hydrophobically modified chitosan were more difficult to remove from the aluminum molds as opposed to scaffolds produced from solutions of unmodified chitosan. The scaffolds were more "fluffy" and cotton like, and some of the hydrophobic scaffolds would tear, because their bottom was firmly attached to the aluminum mold. This observation suggests that the scaffolds from modified chitosan were less rigid than those produced from solutions of unmodified chitosan, and that they also had an enhanced capacity to adhere to the aluminum. SEM images also revealed the presence of small polymer particle precipitates attached to the pore walls. In case of the unmodified chitosan, the surfaces that formed were even and smooth. In case of the butyl-chitosan scaffolds, however, the precipitates formed possessed threads and visible coils. The threads had a diameter of approximately 0.1–0.4μm. The threads appeared to be more elongated and more present at longer freezing times. The pore walls seemed to be thinner and the rims of the pores seemed to be more irregular. Additionally the scaffolds produced from modified chitosan formed a strong surface skin which was hard to cut although the scaffolds seemed to be more fragile than the scaffolds produced from unmodified chitosan. The surface skin of butyl-chitosan scaffolds also possessed more holes which tended to enlarge with increased freezing time and temperature, so that higher freezing temperatures yielded less dense surface skins. The effect of hole formation in the surface skin with increasing freezing time was more significant in scaffolds produced at higher temperature (−5 °C) than at lower temperatures (−20 °C). As a consequence of these observations, scaffolds fabricated from the butyraldehyde modified chitosan (i.e. C4-chitosan) will need to be strengthened if used in the fabrication of porous biocatalytic electrodes. The authors suggest that pretreatment of the chitosan solutions with cross-linking agents (e.g., EDC, GTA) prior to the freezing step will increase strength and have begun experiments to elucidate the effect of cross-linking conditions on both the strength of the resulting scaffold as well as the average pore size (data not shown).

4. Conclusion

In this project the resulting pore size and structure of scaffolds made from both unmodified and hydrophophically modified chitosan were correlated to both freezing time and temperature

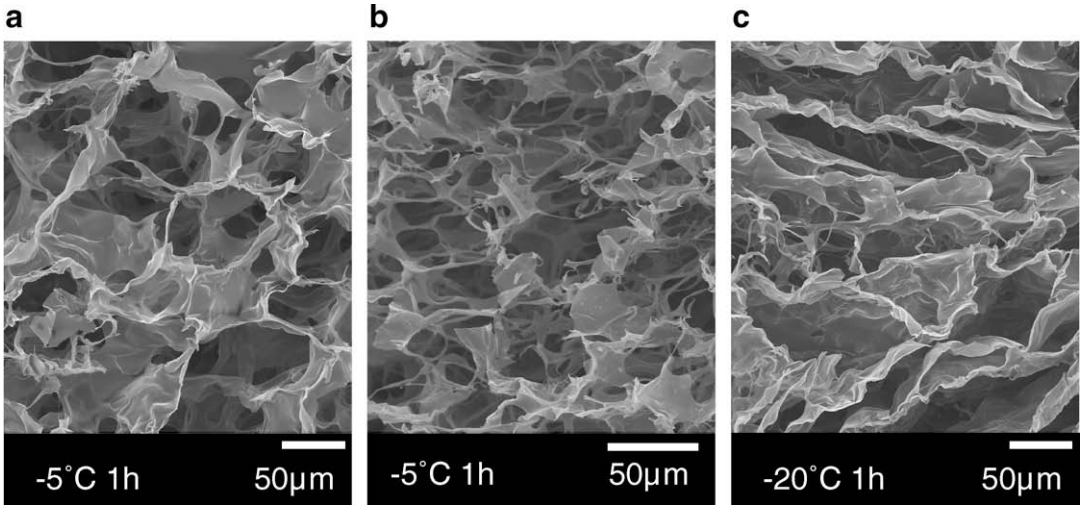

Fig. 10. SEM images of freeze dried scaffolds made from 0.6 wt.% polysaccaride dissolved in 0.2 M HOAc. Image A presents a typical scaffold fabricated from a solution of unmodified chitosan. Image B shows the same except a solution of hydrophobically modified chitosan was used. Image C shows the shift in pore structure (from spherical to longitudinal) observed for the unmodified scaffolds frozen at −20 °C for times longer than 30 min. All chitosan solutions, at different freezing times and temperatures.

(Fig. 10). The modification reaction was found by solid state NMR to be effective. The pore structure of unmodified chitosan scaffolds (Fig. 10a) were highly interconnected and a result of instantaneous nucleation and a phase separation process that was dominated by mass transfer – except at the lowest freezing temperature of −20 °C (Fig. 10c), suggesting that the freezing temperature at which this transition occurs is directly dependent upon the system geometry and how it affects the freezing rate. The pore structure of scaffolds fabricated from the modified chitosan (Fig. 10b) were highly interconnected and a result of progressive nucleation and a phase separation that occurred under mass transfer dominated regime across all freezing temperatures and time. In the context of scaffold formation, the effect of hydrophobically modifying the chitosan was to seemingly extend the conditions of mass transfer dominated growth by raising the freezing temperature (i.e. and lowering ΔT) and therefore mimicking the situation (assuming a fixed amount of total water in the systems) where fewer ice nucleates survive but each ultimately grow larger. Finally, scaffolds fabricated from solutions of hydrophobically modified chitosan were less rigid than those produced from solutions of unmodified chitosan as well as possessing surfaces that were slightly more rough and thread like.

Acknowledgements

Funding for this project was provided by the Office of Naval Research (#00014-06-1-1055, Richard Rocheleau, PI) and Air Force Office of Scientific Research (Sub award from University of New Mexico #986007-873Z, Plamen Atanassov, PI). The authors also thank Dr. Plamen Atanassov for his suggestions regarding both crystal growth and data analysis.

References

Cooney, M. J., Windmeisser, M., Liaw, B. Y., Lau, C., Klotzbach, T., & Minteer, S. D. (2007). Design of chitosan gel pore structure: Towards enzyme catalyzed flow-through electrodes. *Journal of Materials Chemistry*, 10.1039/b7100082e.

Dutta, P. K., Ravikumar, M. N. V., & Dutta, J. (2002). Chitin and chitosan for versatile applications. *Journal of Macromolecular Science-Polymer Reviews, C42*(3), 307–354.

Esquenet, C., Terech, P., Boue, F., & Buhler, E. (2004). Structural and rheological properties of hydrophobically modified polysaccharide associative networks. *Langmuir, 20*(9), 3583–3592.

Gu, Z. Y., Xue, P. H., & Li, W. J. (2001). Preparation of the porous chitosan membrane by cryogenic induced phase separation. *Polymers for Advanced Technologies, 12*(11–12), 665–669.

Heux, L., Brugnerotto, J., Desbrieres, J., Versali, M. F., & Rinaudo, M. (2000). Solid state NMR for determination of degree of acetylation of chitin and chitosan. *Biomacromolecules, 1*, 746–751.

Hsieh, C.-Y., Tsai, S.-P., Ho, M.-H., Wang, D.-M., Liu, C.-E., Hsieh, C.-H., et al. (2007). Analysis of freeze-gelation and cross-linking processes for preparing porous chitosan scaffolds. *Carbohydrate Polymers, 67*(1), 124–132.

Jiang, G. B., Quan, D., Liao, K., & Wang, H. (2006). Preparation of polymeric micelles based on chitosan bearing a small amount of highly hydrophobic groups. *Carbohydrate Polymers, 66*(4), 514–520.

Khvorostyanov, V. I., & Curry, J. A. (2004). The theory of ice nucleation by heterogeneous freezing of deliquescent mixed CCN. Part I: Critical radius, energy, and nucleation rate. *Journal of the Atmospheric Sciences, 61*, 2676–2691.

Klotzbach, T., Watt, M., Ansari, Y., & Minteer, S. D. (2006). Effects of hydrophobic modification of chitosan and Nafion on transport properties, ion-exchange capacties, and enzyme immobilization. *Journal of Membrane Science, 282*, 276–283.

Klotzbach, T. L., Watt, M., Ansari, Y., & Minteer, S. D. (2008). Improving the microenvironment for enzyme immobilization at electrodes by hydrophobically modifying chitosan and Nafion® polymers. *Journal of Membrane Science, 311*(1–2), 81–88.

Lau, C., Cooney, M. J., & Atanassov, P. (2008). Conductive macroporous composite chitosan-carbon nanotube scaffolds. *Langmuir, 24*, 7004–7010.

Leffler, C. C., & Muller, B. W. (2000). Influence of the acid type on the physical and drug release properties of chitosan-gelatin sponges. *International Journal of Pharmaceutics, 194*(2), 229–237.

Li, G., Zhuang, Y., Mu, Q., Wang, M., & Fang, Y. (2008). Preparation, characterization and aggregation behavior of amphiphilic chitosan derivatives having poly(L-lactic acid) side chains. *Carbohydrate Polymers, 72*, 60–66.

Madihally, S. V., & Matthew, H. W. T. (1999). Porous chitosan scaffolds for tissue engineering. *Biomaterials, 20*, 1133–1142.

Methacanon, P., Prasitsilp, M., Pothsree, T., & Pattaraarchachai, J. (2003). Heterogeneous *N*-deacetylation of squid chitin in alkalin solution. *Carbohydrate Polymers, 52*, 119–123.

Penner, R. M. (2001). Mesoscopic metal particles and wires by electrodeposition. *Journal of Physical Chemistry, 2002*(106), 3339–3353.

Roh, I. J., & Kwon, I. C. (2002). Fabrication of a pure porous chitosan bead matrix: Influences of phase separation on the microstructure. *Journal of Biomaterials Science-Polymer Edition, 13*(7), 769–782.